ANALYSIS OF DEEPSTALL LANDING FOR UAV

Hiroki Taniguchi*
***The University of Tokyo**

Keywords: *stall landing, UAV, landing method*

Abstract

Deepstall landing is one of the landing methods by which airplanes can decrease flight speed while maintaining a deep glide path angle. This is because the wing can generate large air drag in the deep stall state. Therefore, the method is suitable for small unmanned aerial vehicle to land within narrow areas surrounded by tall obstacles. This paper considers the trim condition in the deepstall flight phase and a numerical flight simulation from the cruise to the deepstall landing. Furthermore, flight tests were conducted to confirm the deepstall landing characteristics.

1 Introduction

A small unmanned aerial vehicle (UAV) for aerial photography and remote sensing has been developed. In general, the size of a small UAV can range from several tens of centimeters to a few meters, and the propulsion is mostly by an electric powered motor. Ground control software can run on a laptop computer, so the ground station can be set up practically everywhere. Generally, small UAVs are deployed in environments where no access to conventional runways is available, because the UAV can take off by hand launch or catapult, and land at a short distance. Moreover, it is often handled at confined areas surrounded by trees or buildings. It is very difficult to land UAVs at these areas adopting normal glide landing methods, especially for untrained operators. Hence, some effective landing methods must be devised so that the small UAV system can develop into a user-friendly technology.

In these environments, the horizontal speed needs to be decreased and the deep path angle has to be maintained to land safely. To meet this requirement, several solutions have been considered, e.g., parachute landing and vertical take off and landing (VTOL) mechanism. The parachute landing is the most common method because it is easy to operate and the UAV can be retrieved at any time and anywhere. However, it requires a considerable skill to properly fold parachutes and store them in the aircraft body. Furthermore, the parachute itself has large air drag, which makes it difficult to precisely land the UAV at the target point in strong wind conditions. On the other hand, adopting the VTOL method, we can handle UAVs in narrow spaces. However, payload and endurance are limited and high performance controller is necessary as the VTOL system is complicated and originally unstable.

Another way which doesn't suffer from these disadvantages is "deepstall landing", which is studied in this paper. The mechanism is quite simple and it is an effective way to land the planes in narrow space. Because of the large air drag at deep stall, the horizontal speed can be reduced effectively while the deep path angle is kept. Some landing methods taking advantage of stall have been reported in literature [1,2], but deepstall landing method was originally employed to the free flight model plane and has been developed empirically. So, the characteristics of deepstall landing have not been studied precisely.

In this paper, trim state at deepstall landing and the performance as landing method are considered using trim state contour graphs. Numerical flight simulation takes into account the history of attitude and speed from cruise to deepstall phase. A model plane with measuring instruments was developed and a flight test was done to confirm computational results.

2 Deepstall Landing Method

2.1 Characteristics of deep stall

Deep stall is the state in which the angle of attack is much higher than the stall angle. Even though the flow is unstable around the stall angle, it is stable in post-stall. Therefore, the wing can generate constant lift and drag forces when the angle of attack exceeds the stall angle by a certain value. Fig.1 and Fig.2 show the wind tunnel data of a NACA0012 wing [3]. According to Fig.1, the lift coefficient C_L and drag coefficient C_D are larger than at cruise. And Fig.2 means that the value of the lift to drag ratio L/D is smaller in the post stall state than in normal flight.

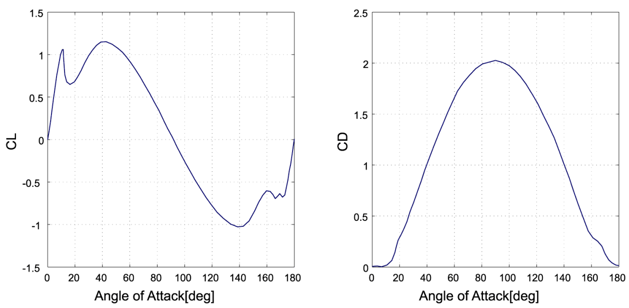

Fig. 1 C_L and C_D data of NACA0012

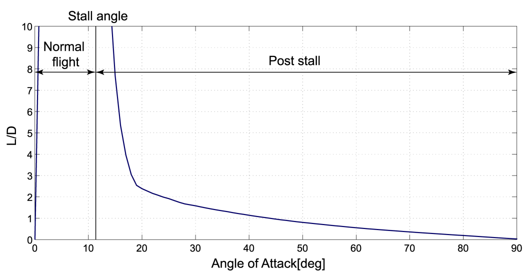

Fig. 2 L/D of NACA0012

2.2 Deepstall Landing Mechanism

The only mechanism to get the plane into deep stall is quickly tilt of the horizontal tail plane (HTP). When the HTP tilts up suddenly at cruise, the plane pitches up largely and the angle of attack gets much higher than the stall angle. Then the plane trims at the deep stall state because the lift of the HTP cancels the wing and body moments. Furthermore, lift of the HTP acts as a restoring force because the HTP is not in stall. Consequently, the plane can keep this stable trim state. In this trimmed deep stall state, C_L and C_D are so large that flight speed is decreased effectively. Besides, the L/D is so small that the plane can keep the deep glide path angle.

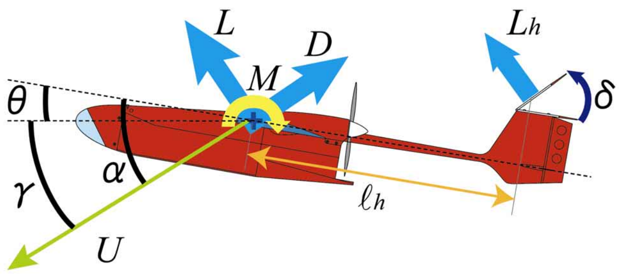

Fig. 3 Model of deepstall landing

2.3 Advantages of Deepstall Landing

The deepstall landing method can be implemented with a simple mechanism of HTP and it has a good stability. Therefore, untrained operators can easily handle it. This is an important point because small UAV system is becoming a platform for aerial photography and remote sensing and in many cases non-skilled operators handle the system. Furthermore, the path angle and speed can be set arbitrarily, controlling the HTP to tilt up by an angle δ. Hence, the landing point can be adjusted in strong wind conditions.

On the other hand, because touch down speed is higher than for the conventional methods, its application may be limited to small UAV only.

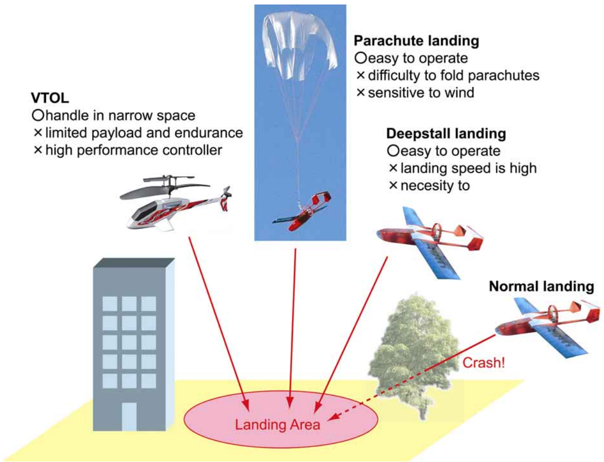

Fig. 4 Characteristics of landing methods for small UAV system

3 Trim State Analysis

3.1 Equations of Equilibrium

Firstly, longitudinal trim conditions in the phase of deepstall landing were estimated. The trim state of an aircraft can be expressed by the following three equations:

$$L\cos\gamma + D\sin\gamma = M\cdot g \quad (1)$$

$$L\sin\gamma - D\cos\gamma = 0 \quad (2)$$

$$M - L_h\cdot l_h\cdot\cos(\alpha_h+\delta) = 0 \quad (3)$$

Variables are defined in Fig.3. Constant number g is a gravitation constant. Variables with suffix h are the value for the HTP. Lift and drag forces and moment can be modeled as functions of the angle of attack referring to NACA0012 wind tunnel data which includes after stall data. The moment balance equation (3) is expressed as below applying HTP volume V_h as variable.

$$C_M - V_h\cdot C_{Lh}\cdot\cos(\alpha_h+\delta) = 0 \quad (4)$$

$$V_h = \frac{l_h\cdot S_h}{c\cdot S} \quad (5)$$

Therefore, the trim state can be determined once V_h and δ are fixed.

3.2 Calculation Conditions

The plane model is based on a existing free flight plane, which weighs 230*g*, and wing span is 1.4*m* long. The plane has a pop up mechanism of the HTP and deepstall landing has been realized. Its details are summarized in Table.1. In this analysis, trim state was calculated under the condition that V_h and δ were the variable and weight M and wing area S were constant.

Table. 1 Configuration of the model free flight plane

General		Main wing		
M weight *(kg)*	I_{yy} inertia moment *(kg m²)*	b span (m)	S wing area (m^2)	AR aspect ratio
0.231	0.00622	1.38	0.159	12
HTP				
b_h span (m)	S_h wing area (m^2)	l_h ※1 (m)	AR aspect ratio	V_h HTP volume
0.337	0.0256	0.635	4.43	1.12

※1 expressed in Fig.3

3.3 Contour Lines of Trim State

Fig.5 to 7 show the contours of the attitude and speed at trimmed deepstall landing phase. Horizontal and vertical axes of the graphs show V_h and δ respectively. Fig.5 shows the pitch angle contour lines at the final deepstall state. The red lines mean that pitch angle is 0° and the plane can land horizontally. However, the pitch angle is less than 6° in most cases, so the plane can land almost horizontally in any configurations. Final velocity decreases as V_h and δ increase. This happens because the angle of attack becomes larger at higher V_h and δ. Fig.7 shows the final vertical speed and path angle contours. These are important parameters to measure the performance of deepstall landing because vertical velocity directly defines the impact to the body and path angle decides the size of area necessary to land. The deepstall constraint line was added because the angle of attack is smaller than the stall angle below the line. As tilt up angle δ increases, vertical speed becomes larger but the deep path angle can be maintained. Therefore, an optimal configuration must be chosen depending on the landing area environments and damage to the body.

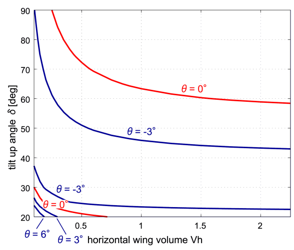

Fig. 5 Pitch angle

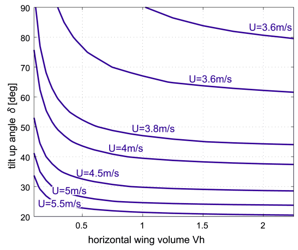

Fig. 6 final absolute speed

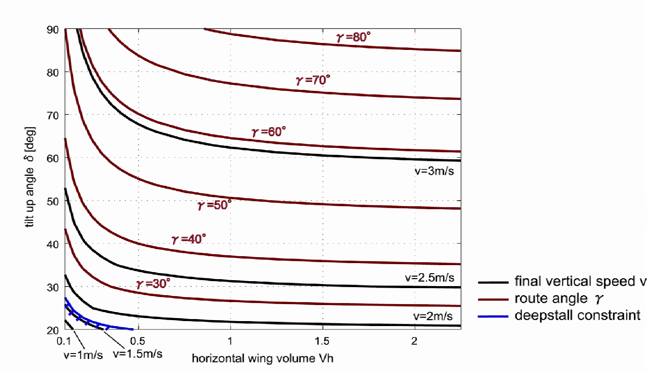

Fig. 7 Performance curve of deepstall landing

4 Flight Simulation

In the next step, transition flight from the cruise into the deepstall landing was simulated in a flight simulator developed in MATLAB/Simulink. It considers the flight in the longitudinal plane only. As in the trim analysis, lift and drag forces and moment are modeled using NACA0012 wind tunnel data.

Fig.8 shows the resulting trajectories of the airplane when the HTP is tilted up 25° , 35° , 45° and 55° respectively. Plane figures plotted every 0.5 second show the position and attitude of the plane. The HTP is tilted up after 1.0 second and simulations are carried out until 10 second. As described in section 2, the glide path angle is larger at higher tilt up angle. These results indicate that first the airplane pitches up, then it pitches down and it comes to be nearly horizontal in the end. Fig.9 shows the speed and the angle of attack, pitch and path angle histories when the tilt up angle δ is 45° . It takes about 2.5 seconds to converge to the final trim state, which means the attitude of the plane can stabilize quickly.

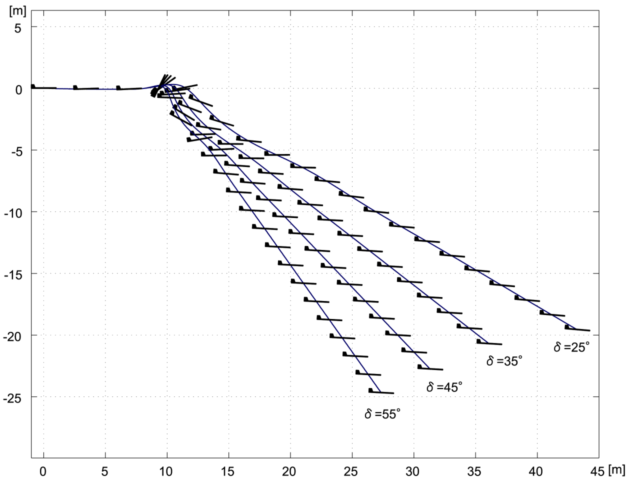

Fig. 8 Trajectories and attitudes of the deepstall simulation

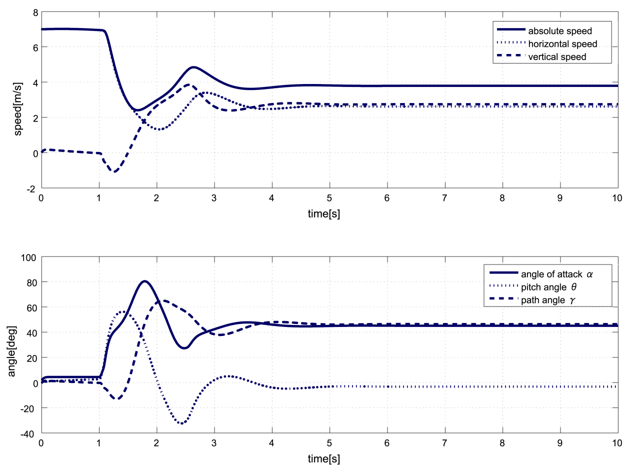

Fig. 9 Speed and angle histories at 45° tilted up

5 Analysis Result of Real Flight Tests

Flight tests were conducted to confirm the characteristics of deepstall landing in real flight. Flight data was obtained and it was compared with the simulation results.

5.1 Test plane

The shape of the test plane is similar to the model free flight plane used in the computational simulation. The configuration of the plane is summarized in Table 2. It is a motor powered glider, with the HTP fixed to the body by a high precision servomotor. Therefore, the wing can be tilted up arbitrarily from −5° to 50° by pilot commands. A flight logger, which was composed of 3 gyros, 3 accelerometers and a GPS receiver, was fixed in the plane. It had been developed in the laboratory and the accuracy had been confirmed [4]. As a result, attitude, speed, and position history data were recorded.

Fig. 10 Test plane

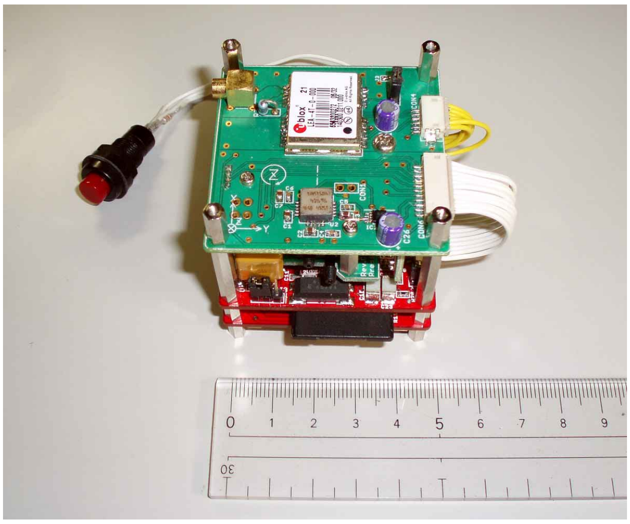

Fig. 11 Flight logger installed in the test plane

Table. 2 Configuration of the test plane

General		Main wing		
M (kg)	I_{yy} (kg m^2)	b (m)	S (m^2)	AR
0.498	0.0227	1.52	0.190	12
HTP				
b_h (m)	S_h (m^2)	l_h (m)	AR	V_h
0.37	0.0315	0.603	4.35	0.828

5.2 Flight Test data

Using this test plane, a flight test was conducted and data could be obtained successfully. Fig.12 shows the 3D trajectory and plane attitude of flight test. The HTP tilt up angle δ was 35° . The plane direction was rotating as the roll angle was not equal to zero, because the HTP was accidentally fixed with a little tilt. Fig.13 shows the trajectory and attitude projected on the longitudinal plane. When the HTP was tilted up, the plane pitched up and then down, and it converged to the horizontal trim state. Fig.14 shows the speed and attitude time histories. Blue lines are flight test data and red ones are simulation results. The same trend is observed in the flight test data and the simulation results discussed in section 4. The value of the glide path angle is a little different between the anterior half and posterior half of the deepstall phase. This could be because the wind direction relative to the plane changed because the plane was rotating.

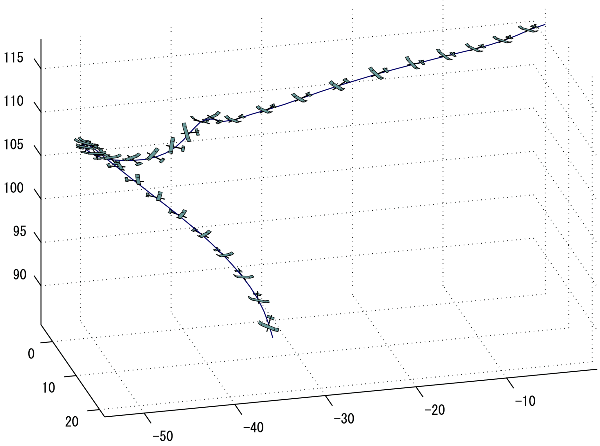

Fig. 12 3D plot of flight trajectory and the plane attitudes

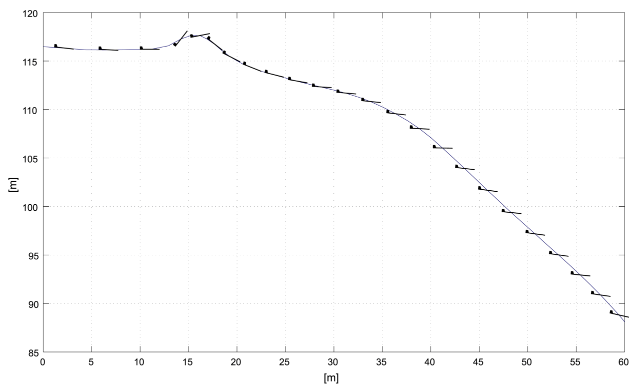

Fig. 13 Trajectory and the plane attitude projected on longitudinal plane

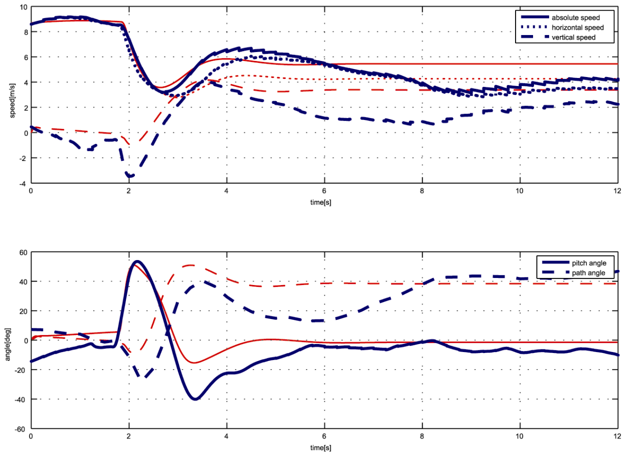

Fig. 14 Speed and angle histories of real flight test and simulation result

6 Conclusions

Adopting deepstall landing method, the plane can decrease the flight speed effectively and maintain the deep path angle. These advantages were confirmed through trim analysis. Using the trim plot (Fig.7), the values of V_h and δ can be decided for a certain path angle, steep enough to land in a confined area and which result in a vertical speed low enough to prevent damage of the body. The longitudinal transition phase from steady flight to deepstall landing was simulated and an adequate dynamical stability was observed. Finally, a real flight test was conducted and the flight data support that the trim analysis and flight simulation are effective to estimate the dynamical characteristics and performance of deepstall landing. In a future study, more research about longitudinal and lateral stability will be done and UAV design that is optimal for deepstall landing will be considered.

References

[1] Crowther W. Perched Landing and Takeoff for Fixed Wing UAVs. *NATO AVT Symposium on Unmanned Vehicles for Aerial, Ground and Naval Military Operations*, 2000 (Report #RTO-MP-052).

[2] Crowther W, Prassas K. Post-stall landing for field retrieval of unmanned air vehicles. *14th Bristol International unmanned air vehicle systems conference*, April 1999 (Paper #39).

[3] Critzos C, Heyson H, Boswinkle, Aerodynamic characteristics of NACA0012 airfoil section at angles of attack from 0° to 180° , NACA TECHNICAL NOTE 3361, 1955.

[4] Naruoka M. Attitude accuracy improvement of ultra low-grade MEMS INS using alignment of GPS antenna. *26th Congress of International Council of Aeronautical Sciences (ICAS 2008)*, Anchorage, 2008.

Copyright Statement